Rietveld refinement for indium nitride in the 105–295 K range

W. Paszkowicz[a)]
Institute of Physics, Polish Academy of Sciences, Al. Lotnikow 32/46, 02-668 Warsaw, Poland

R. Černý
University of Geneva, Laboratory of Crystallography, 24 Quai E. Ansermet, CH-1211 Geneva 4, Switzerland

S. Krukowski
High-Pressure Research Centre, Polish Academy of Sciences, 01-142 Warsaw, ul. Sokołowska 29/37, Poland

(Received 8 June 2002; accepted 13 February 2003)

Results of Rietveld refinement for indium nitride data collected in the temperature range 105–295 K are presented. Acicular microcrystals of indium nitride prepared by reaction of liquid indium with nitrogen plasma were studied by X-ray diffraction. The diffraction measurements were carried out at the Swiss-Norwegian Beamline SNBL (ESRF) using a MAR345 image-plate detector. Excellent counting statistics allowed for refinement of the lattice parameters of InN as well as those of the metallic indium secondary phase. In the studied temperature range, the InN lattice parameters show a smooth increase that can be approximated by a linear function. Lattice-parameter dependencies confirm the trends indicated earlier by data measured using a conventional equipment. The relative change of both the *a* and *c* lattice parameters with increasing the temperature in the studied range is about 0.05%. The axial ratio slightly decreases with rising temperature. The experimental value of the free structural parameter, $u=0.3769(14)$, is reported for InN for the first time. Its temperature variation is found to be considerably smaller than the experimental error. The thermal-expansion coefficients (TECs), derived from the linearly approximated lattice-parameter dependencies, are $\alpha_a=3.09(14)\times10^{-6}$ K^{-1} and $\alpha_c=2.79(16)\times10^{-6}$ K^{-1}. The evaluated TECs are generally consistent with the earlier data. For the present dataset, the accuracy is apparently higher for both, the lattice parameters and thermal-expansion coefficients, than for the earlier results. The refined lattice parameter c_{In} of the indium secondary phase exhibits the known strongly nonlinear behavior; a shift (ΔT equal about -50 K) of the maximum in $c_{\mathrm{In}}(T)$ dependence is observed with respect to the literature data. © *2003 International Centre for Diffraction Data.* [DOI: 10.1154/1.1566957]

Key words: thermal expansion, inorganic compound, nitride, III-V semiconductor, indium

I. INTRODUCTION

Indium nitride is a semiconductor [with earlier assumed direct energy gap of value 1.89 eV, after Tansley and Foley (1986); now thought to be about or below 1 eV, see Inushima *et al.* (2001); Wu *et al.* (2002); Bechstedt and Fürthmüller (2002)] that has applications as a component of pseudobinary thin III-V layers (such as InGaN and InGaAlN) in modern short-wavelength optoelectronic devices. Using indium in solid solutions allows for tuning of the (direct) energy gap and lattice parameters over a broad range. Also, using InN as a solution component allows tuning of the thermoelastic properties of the solution. One of the achievements in the field of III-V based optoelectronics is the continuous-wave operation of (In,Ga)N multi-quantum-well structure laser diodes with a long lifetime (Nakamura, 1999). Additionally, the presence of indium was recently found to greatly improve the optical efficiency of nitride-based light emitting diodes (LEDs) and laser diodes; the nature of this effect is under study (Nakamura, 2000a, 2000b; Chichibu *et al.*, 2000; Godlewski and Goldys, 2001). A growing interest in applications resulted in a rapidly growing number of papers devoted to this compound family [number of papers involving these compounds increased by two orders of magnitude in 26 years, as shown by Monemar (1999)].

Indium nitride, InN, is a compound difficult to synthesize from both the vapor and liquid phase. Vapor based crystal growth methods are not applicable when the difference in vapor pressures or in melting points is too great. Growth from solution fails because the equilibrium pressure of nitrogen is very high and limits the possible growth temperatures (Grzegory *et al.*, 1993a, 1993b, 1994). Additionally, the kinetic barriers prevent dissolution of nitrogen in liquid indium, and thus prevent InN synthesis (Krukowski *et al.*, 1998a; Romanowski *et al.*, 2001). So far, bulk InN has been synthesized effectively either by chemical methods (Goryunova, 1965; McChesney *et al.*, 1970; Podsiadlo, 1995), by reaction of the components or by reaction of molten indium with nitrogen plasma (RNP) (Angus *et al.*, 1997; Krukowski *et al.*, 1998b). Chemical methods lead to higher impurity levels in the crystals, which cause poor crystallographic quality. The RNP method is accompanied by difficulties in controlling the growth conditions; this may lead to small size and deterioration of the crystallographic quality of the material.

The InN crystal structure is of wurtzite type (space group $P6_3mc$). Thin layers also can be grown with the zincblende structure type. Reported room-temperature lattice

a) Electronic mail: paszk@ifpan.edu.pl

TABLE I. For a comment concerning the lattice parameter error see text. Lattice parameters *a*, *c*, unit cell volume, *V*, axial ratio, *c/a*, for the wurtzite-type InN. (The values of *V*, *c/a*, were calculated from cited *a* and *c* values if not given in the reference.) In each of groups, the data are chronologically ordered. "MV" denotes samples prepared by microwave plasma method. The following abbreviations are used to designate the theoretical models: PP—pair potential method, LMTO—linear muffin-tin orbital, LDA—local density approximation, CGA—generalized gradient approximation, HF—Hartree–Fock, PWPP—plane-wave pseudopotential, SE—semiempirical model, and VCM—various calculation methods. "rt" refers to room temperature.

No.	*T* (K)	*a* (Å)	*c* (Å)	*V* (Å^3)	*c/a*	*u*	Reference	Remarks
				Experimental data (bulk crystals)—wurtzite structure				
1	rt	3.540	5.704	61.90	1.6113		Juza and Hahn (1938)	
2	rt	3.54	5.71	62.0	1.613		MacChesney *et al.* (1970)	
3	rt	3.544	5.718	62.20	1.613		Osamura *et al.* (1975)	
4	rt	3.529(5)	5.694(5)	61.4(2)	1.613(4)		Sheleg and Sevastenko (1976)	
5	296(3)	3.5376(3)	5.7036(5)	61.81(2)	1.6123(3)		Juza and Hahn (1938)	MV, sample S3
6	rt	3.5366(5)	5.7009(5)	61.75(2)	1.6120(4)		Dyck *et al.* (1999)	MV
7	295(1)	3.53774(18)[a]	5.7037(4)[a]	61.821(11)[a]	1.61224(20)[a]	0.3769(13)	This work	MV, sample S3
				Experimental data (layers)—wurtzite structure				
8	rt	3.5446	5.7034	62.058	1.6090		Pichugin and Tlachala (1978)	epitaxial layer
9	rt	3.5480(5)	5.7600(5)	62.79(2)	1.6234(3)		Tansley and Foley (1986)	thin film
10	rt	3.540	5.705	61.91	1.612		Kubota *et al.* (1989)	epitaxial layer
11	rt	3.6	5.74	64.4	1.59		Strite *et al.* (1993)	epitaxial layer
				Theoretical data—wurtzite structure				
12	rt	3.536	5.709	61.818	1.615	0.380	Yeh *et al.* (1992)	LDA
13	rt	3.483	5.7039	59.93	1.638	0.3767	Munoz and Kunc (1993)	PP
14	rt	3.501	5.669	60.176	1.619	0.3784	Wright and Nelson (1995)	PWPP
15	rt				1.644	0.3749	Besson *et al.* (1996)	LDA
16	rt	3.53	5.54	59.8	1.57	0.388	Kim *et al.* (1996)	LMTO
17	rt	3.5428	5.7287	62.27	1.6170	0.3784	Paulus *et al.* (1997)	HF
18	rt	3.53	5.69	61.40	1.6119		Chisholm *et al.* (1999)	
19	298	3.53743	5.70273	61.800	1.6121		Wang and Reeber (2001)	semiempirical model
20	rt	3.509	5.657	60.32	1.6121	0.3791	Zoroddu *et al.* (2001)	LDA
	rt	3.5848	5.8002	64.551	1.6180	0.37929		CGA
21	rt	3.544/3.614 [3.50-3.61]	5.762/5.884 [5.54-5.88]	62.67/66.55 [58.8-66.4]	1.626/1.628 [1.57-1.63]	0.377/0.377 [0.375-0.388]	Stampfl and Van de Walle (1999) [reviewed]	LDA/CGA [various calculation methods]
				Experimental data (layers)—ZB structure				
22	rt	4.98(1)		123.5(7)			Strite *et al.* (1993)	epitaxial layer
23	723	5.04(9)		128(7)			Lima *et al.* (1999)	epitaxial layer
24	rt	4.97		122.7			Tabata *et al.* (1999)	epitaxial layer
25	rt	4.98(1)		123.5(7)			Lima *et al.* (1999)	epitaxial layer
26	rt	5.09(4)		132(3)			Bhattacharya *et al.* (2002)	thin film
				Theoretical data—ZB structure				
27	rt	4.9870		124.0			Paulus *et al.* (1997)	HF
28	rt	4.92		119.1			Kim *et al.* (1996)	LMTO
29	rt	4.964 /5.109		122.3 /133.4			Zoroddu *et al.* (2001)	LDA /CGA
30	rt	4.92-5.109		119.1-133.4			theoretical values reviewed in Stampfl and Van de Walle (1999) and Tabata *et al.* (1999)	various calculation methods

parameters of InN are collected in Table I for both structure types.

Thermal expansion of each material used for optoelectronic device construction is a factor influencing the properties of the product through the thermal strain. In particular, for $In_{1-x}Ga_xN$ and $In_{1-x-y}Ga_xAl_{1-y}N$ solid solutions, the knowledge of thermal expansion is helpful in determination of the layer composition. Therefore, detailed studies of InN thermal expansion may be useful in designing and improving the technologies involving this material as a component. It has been reported that heteroepitaxial growth of wurtzite-type GaN or InGaN starts through growth of zincblende islands; this phenomenon can be observed *in situ* (see, e.g., Wu *et al.*, 1996; Li *et al.*, 1998; Kim *et al.*, 2002). It clearly shows that for any III-V nitride, the elastic properties of both, zincblende and wurtzite, polytypes have to be studied.

InN is known to exhibit relatively low thermal expansion, comparable to that of other III-V nitrides. Very limited information about InN expansivity can be found in literature. According to the first published experimental data (Sheleg and Savastenko, 1976; see also Tansley, 1994) available for the range 190–560 K, the TECs increase with temperature: α_a from 3.4×10^{-6} K^{-1} to 5.7×10^{-6} K^{-1}, α_c from 2.7×10^{-6} K^{-1} to 3.7×10^{-6} K^{-1}. Recent studies include an experimental work on lattice parameters and thermal expansion (Paszkowicz *et al.*, 1999, hereafter referred to as Ref. I), and calculations based on a semiempirical model (Wang and Reeber, 2001). The data of Ref. I concern the expansion in the 100–673 K range based on diffraction data collected with a conventional laboratory instrument. Average TECs determined for this range are $\alpha_a = 3.6(2)\times10^{-6}$ K^{-1} and

https://doi.org/10.1154/1.1566957

$\alpha_c = 2.6(3) \times 10^{-6}$ K^{-1}. Due to the scatter of experimental points obtained with the use of conventional equipment, there is a lack of detectable TEC variation in the investigated temperature interval for these data, in contrast to the dependencies reported, in a smaller range, by Sheleg and Savastenko, (1976). In the most recent work (Wang and Reeber, 2001) the lattice parameters and TECs have been calculated in the range 50–800 K based on a semiempirical model. For a zincblende-type indium nitride layer, a lattice-parameter value at 723 K has been reported (Lima *et al.*, 1999); due to a large error (0.09 Å), this result cannot be used for reliable evaluation of the TEC for the zincblende polymorph. The dependence of the lattice-parameters on temperature can be concluded to be not known accurately. Therefore, a new experimental effort was justified.

An intense synchrotron X-ray beam combined with 2D detectors allows collection of data with counting statistics suitable for performing highly accurate structural analysis. In order to demonstrate the improvements of data quality enabled by the intense incident beam, in this work the results of Rietveld refinement of InN powder diffraction patterns in the temperature range 105–295 K collected at a third-generation synchrotron radiation source are presented. The obtained results include the lattice parameter dependence on temperature and averaged TECs for indium nitride.

II. EXPERIMENTAL

Fine InN powder was synthesized at the High-Pressure Research Center, Warsaw, by reaction of liquid indium with nitrogen plasma in a vertical microwave plasma reactor [for preparation details see Krukowski *et al.*, 1998b and Ref. I]. The material selected for this study was the sample S3 characterized in Ref. I.

For the purpose of crystallite-orientation analysis, additional patterns were collected (CuKα radiation) using a laboratory Bragg-Brentano diffractometer. To reveal the crystallographic orientation of the side faces of the acicular InN crystals, a small quantity of the powder was spread using a drop of ethyl alcohol on a flat plexiglas holder. The crystallographic long axis of the crystallites was determined using the same procedure for a holder differing from the standard one by parallel 0.2 mm wide grooves of triangular cross-section machined on its surface. The grooves were filled by the powder, a drop of alcohol helped in alignment of the needles along the grooves, and the side face of this holder was mounted as a sample for the Bragg-Brentano measurement. Only a small quantity of needles ''standing'' at the side face could effectively diffract. Nevertheless, the signal was strong enough to be helpful in analysis of the crystallite orientation.

The X-ray diffraction measurements were made at the Swiss-Norwegian Beamline BM1A of the European Synchrotron Radiation Facility, Grenoble, using Debye-Scherrer geometry. For data collection, a MAR345 image plate (IP) with 150×150 μm^2 pixel size was employed. The beam size on the sample was 0.5×0.5 mm^2 and the sample to detector distance was 120 mm. The wavelength (0.698670 Å) and the IP position were calibrated using NIST 640b silicon standard, $a = 5.43094$ Å. The InN powder was mounted in a (stationary) sealed thin-wall (0.01 mm) boron-glass capillary of

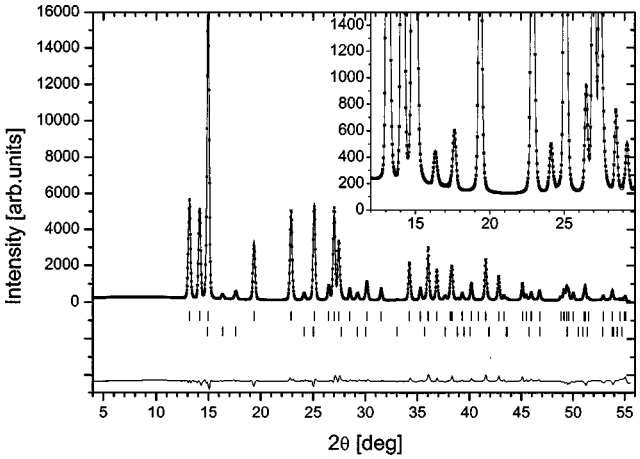

Figure 1. Result of Rietveld refinement for a powder diffraction pattern of InN (data collected at $T = 105$ K using wavelength equal 0.698 670 Å). Crosses denote experimental points, and the solid line is the calculated pattern. Calculated reflection positions for the main InN phase and the In secondary phase are marked below the pattern using vertical bars (upper and lower row, respectively). The difference pattern is shown in the lower part of the figure. The inset illustrates the refinement quality for the In secondary phase (all untruncated peaks in the inset belong to the In phase).

0.4 mm inner diameter. The temperature (105–295 K) was controlled by an Oxford Instruments Cryostream apparatus and kept constant within 1 K. The measurements were performed at increasing temperature using 30 to 40 K temperature steps. Typically, a delay of 5 min was used for the temperature stabilization. One powder pattern was collected in 15 s.

The images were integrated to one-dimensional powder patterns using the FIT2D program (Hammersley, 1995) within the angular range 10–55° (2θ). The integrating procedure included a polarization correction. The Rietveld-refinement program Fullprof.2k v.1 (Rodriguez-Carvajal, 2001) was used for the structural analysis. A pseudo-Voigt profile-shape function was assumed. The following parameters (total 26) were refined by the Rietveld procedure: lattice parameters of both phases, profile parameters, free positional parameter of InN, and six background parameters. The zero-shift parameter was fixed at a value common for all temperatures, because there is no physical reason to vary it during a single series of measurements. Preferred orientation parameters were not refined in the final refinements, as taking them did not lead to improvement. The lattice parameters of the indium secondary phase could be studied owing to excellent counting statistics. For this phase, the peak width parameters and the scale factor were refined independently. The errors for the refined parameters are the standard deviations yielded by the refinement program.

III. RESULTS AND DISCUSSION

A. Morphology and orientation of crystal axis and faces

The phase analysis confirmed that, as for other samples described in Ref. I, the studied sample contains a metallic-indium secondary phase which gives diffraction peaks of weak (several percent) intensity; no other phase was detected (see Figure 1). The crystal morphology was revealed by op-

https://doi.org/10.1154/1.1566957

Figure 2. Crystallites of InN (sample 3) seen under optical microscope in transmission mode.

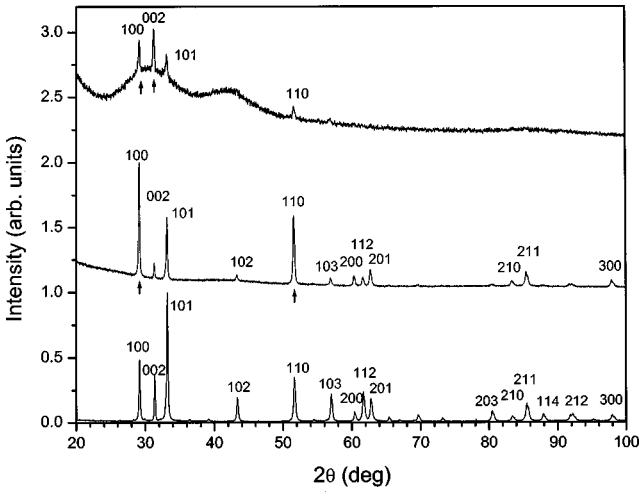

Figure 3. Powder diffraction patterns (collected using CuKα radiation) for crystallites oriented randomly (lower curve) and in the axial (middle curve) and parallel (upper curve) positions. The arrows mark particularly strong reflections that indicate the dominant axis or face orientations.

tical microscopy: long needles, 1–10 μm thick, with a length larger by an order of magnitude (see Figure 2). Their regular shape suggests that at least a large part of them are single crystals. Their morphology is different from that for microcrystals prepared by a related method by Angus *et al.* (1997) (small facetted crystals) and by Dyck *et al.* (1999) (dendritic and platelet type morphology). Among the InN needles, tear-shaped indium droplets were seen. The above observations can be compared with the results of earlier studies on whisker growth of III-V nitrides. For InN, very limited data are available (Mamutin, 1999; Parala *et al.*, 2001). Parala *et al.* (2001) reported CVD growth of InN whiskers at 773 K on a sapphire substrate, with a thickness of 0.1–0.5 μm and lengths exceeding 10 μm. These whiskers from the latter reference have tips ending with indium droplets; the relative intensity of the indium-phase reflections is similar to that measured for our sample. The needles in our sample are more uniform in size and larger than these whiskers.

Results of laboratory experiments with crystallites aligned in the sample holder plane and vertically to it are shown in Figure 3. Numerical values of reflection intensities are compared to the literature data in Table II. As shown in Table II, the data for a virtually randomly oriented powder are consistent with earlier reported patterns. For the elongated shape, one can assume that a considerable fraction of needles was aligned with the holder surface or along the grooves, causing dramatic changes in the measured peak intensities.

Figure 3 shows that the dominant needle axis is [001] (the strongest intensity increase relative to the random case), while the side faces of the needles are mostly (100), (110) and (201). A similar [001] whisker-axis orientation can be deduced from the diffraction pattern by Parala *et al.* (2001), where the 002 reflection is particularly strong (whiskers tend to grow vertically to the substrate surface), cf. Table II. A number of methods lead to whiskers or acicular crystals for AlN (Tanaka *et al.*, 1997; Zhou *et al.*, 2000; Vaidhyanathan *et al.*, 2000; Bockowski, 2001), and for GaN (Elwell *et al.*, 1984; Prywer and Krukowski, 1998; Mamutin, 1999). The present finding of [001] orientation of the long axis of InN crystals correlates with the most frequently observed direction reported for III-V nitride microcrystals. It is noteworthy that the growth of AlN whiskers may be affected by oxygen impurity (Miao *et al.*, 1997; Wang *et al.*, 2001); the grain shape in thin films is known to be dependent on the presence of hydrogen (Lee *et al.*, 1995). Thus, it seems possible to deduce the presence of certain impurities from the III-V nitride crystallite shape.

B. Lattice parameters and thermal expansion

A powder pattern collected at 105 K is shown as an example in Figure 1, together with the refined pattern. The R_p and R_{wp} factor values were in the ranges 5.0%–5.3% and 9.0–9.4, respectively, for the studied patterns at the end of refinement. The inset presents a low angle part of the diffractogram illustrating the high quality of refinement of the indium secondary phase. The differential intensity plot shows the good quality of the refinement. The intensities observed in this study, which employed the Debye-Scherrer method, marginally differed from those determined using Bragg-Brentano diffraction geometry (cf. Table II). This agreement occurs despite the acicular morphology of the microcrystals, showing that the efforts to minimize preferred orientation, together with the preferred orientation correction applied in the refinement (for the Bragg-Brentano data), were successful. This conclusion is consistent with the lack of improvement when attempting to refine the preferred orientation parameter for the studied sample.

The refined structural data of InN are given in Table III. Those at 295 K, a=3.5377(2) Å and c=5.7037(4) Å, are consistent with earlier data (cf. Table I). The room-temperature lattice-parameter values of InN are identical (within the error margins) to the data for the same sample given in Ref. I. A comparison with the literature shows that, in general, there is a satisfactory agreement of lattice parameters between the present and reported experimental and theoretical data determined at room temperature. In particular, the discrepancy with a sample independently prepared by the same method in another laboratory (Dyck *et al.*, 1999) is quite small (about Δa=0.001 Å, Δc=0.003 Å).

The value of the room temperature atomic positional parameter, resulting from the refinement, u=0.3769(13), gen-

https://doi.org/10.1154/1.1566957

TABLE II. Intensities of selected Bragg peaks for indium nitride measured using different geometries. Abbreviations: I_{DS}—intensity measured by a Debye Scherrer method, I_{BB}—intensity measured by a Bragg Brentano method, ''face''/''axis''—needles (whiskers) mounted parallelly/vertically to the sample holder surface, ''random''—sample preparation in a random way. ''w'' and ''nd'' denote weak and not detected peaks (respectively). Intensities of reflections that are particularly strong/weak in respect to the patterns of random samples (or calculated pattern) are indicated by underlined **bold**/*italic* font. The numerical data from the work by Parala *et al.* (2001) were evaluated from a figure in the cited paper.

h k l	d (A)	Calculated (random) (PDF 79-2498)	I_{BB} (random) sample S3 (Paszkowicz, 1999)	I_{DS} (random) sample S3 (this work)	I_{BB} (axis) (Parala, 2001)	I_{BB} (axis) sample S3 (this work)	I_{BB} (face) sample S3 (this work)
1 0 0	3.065	37	44	34	35	**137**	**181**
0 0 2	2.853	32	41	31	**74**	**187**	25
1 0 1	2.700	100	100	100	100	100	100
1 0 2	2.088	17	24	19	*7*	*w*	22
1 1 0	1.769	22	50	30	23	50	**108**
1 1 2	1.503	19	40	31	*9*	*nd*	30
2 0 1	1.480	12	30	19	*6*	*w*	**60**

erally agrees with the theoretical data obtained by the LDA $u=0.3749$ (Besson *et al.*, 1996), by the PP method, $u=0.3767$ (Muñoz and Kunc, 1993), by the LDA and CGA methods, $u=0.377$ (Stampfl and Van de Walle, 1999) and $u=0.379$ (Zoroddu *et al.*, 2001), (note also the perfect agreement of the axial ratio with the experiment for the LDA case), by the PWPP method, $u=0.3784$ (Wright and Nelson, 1995), and by the HF method, also $u=0.3784$ (Paulus *et al.*, 1997). No published experimental data exist. Earlier reported theoretical u values for InN have been reviewed by Stampfl and Van de Walle (1999), they range from 0.375 to 0.388 (most frequently from 0.377 to 0.380). Our experience for InN shows that Rietveld refinement of laboratory Bragg-Brentano data collected with poor statistics yields overestimated u values of about 0.39–0.40, which tend towards more reliable lower values if the statistics are improved.

The variation of InN lattice parameters with temperature is shown in Figure 4. The dependence is found to be smooth for both a and c. It can be satisfactorily approximated by the following formulas:

$$a(T)=3.5345(1)+1.09(5)\times10^{-5}T, \quad (1)$$

$$c(T)=5.6989(2)+1.59(9)\times10^{-5}T. \quad (2)$$

The relative change of both a and c lattice parameters with increasing (in the studied range) temperature is about 0.05%. Earlier data are also shown in Figure 4, including the unpublished preliminary $a(T)$ results (range 10–297 K) collected at the B2 beamline, Hasylab/DESY, Hamburg (Paszkowicz and Knapp, 1999, hereafter referred to as Ref. II), for another indium nitride sample.

The axial ratio illustrated in Figure 3 smoothly decreases with increasing temperature, confirming the tendency observed (in a larger range) in Ref. I. The observed decrease rate is markedly smaller (relative change as low as 5×10^{-5} in the studied temperature range, i.e., below the standard deviation of a single point) than that obtained from the semiempirical model (Wang and Reeber, 2001). The axial ratio has been also studied for III-V nitrides as a function of increasing pressure at a fixed room temperature: a decrease of c/a has been found theoretically for AlN (Christensen and Gorczyca, 1993) and experimentally for InN (Ueno *et al.*, 1994). The decrease of c/a with increasing both p and T may indicate that both these factors enhance the ionicity of the chemical bond in wurtzite-type III-V nitrides.

Relative temperature changes of the free structural parameter, u, are of the order of 4×10^{-4} with a decreasing tendency on increasing temperature, but the variation is much smaller than the standard deviation of a single point More certain detecting of systematic changes of u with temperature would perhaps be easier in a much larger temperature interval. As far as we know, the temperature effect on u has not been experimentally determined for any of III-V nitrides. Only a pressure effect has been calculated. For InN, Besson *et al.* (1996) have predicted that u should increase

TABLE III. Rietveld refinement results: lattice parameters a and c, axial ratio, c/a, volume, V, and positional parameter u for wurtzite-type InN, and a and c values for the In secondary phase as a function of temperature. Statistical refinement errors are indicated. Coefficients of polynomial fitting of all parameters, A_i , are also given.

	InN					*In*			
T	a	c	c/a	V	u	a	c	c/a	V
105	3.535 55(18)	5.7005(4)	1.612 32(20)	61.710(11)	0.3773(13)	3.2377(3)	4.9342(7)	1.6965(3)	44.794(14)
135	3.536 09(18)	5.7013(4)	1.612 32(20)	61.738(11)	0.3775(13)	3.2387(3)	4.9368(7)	1.6981(3)	44.847(14)
175	3.536 40(17)	5.7018(4)	1.612 31(20)	61.754(11)	0.3774(13)	3.2409(3)	4.9391(7)	1.6982(3)	44.927(14)
215	3.536 77(18)	5.7023(4)	1.612 29(20)	61.772(11)	0.3771(13)	3.2446(3)	4.9398(8)	1.6952(3)	45.037(14)
255	3.537 23(18)	5.7029(4)	1.612 26(20)	61.796(11)	0.3770(13)	3.2495(3)	4.9390(8)	1.6895(3)	45.165(14)
295	3.537 74(18)	5.7037(4)	1.612 24(20)	61.821(11)	0.3769(13)	3.2549(3)	4.9371(9)	1.6821(3)	45.299(14)
A_0	3.53449(11)	5.69894(19)	1.612 225(5)	61.656(6)	0.3777(1)	3.2390(8)	4.9187(4)	1.6797(11)	44.691(17)
A_1	$1.09(5)\times10^{-5}$	$1.59(9)\times10^{-5}$	$1.77(9)\times10^{-6}$	$5.5(3)\times10^{-4}$	$-2.8(7)\times10^{-6}$	$-5.0(8)\times10^{-5}$ T	$1.94(4)\times10^{-4}$	$2.44(12)\times10^{-4}$	$3.7(19)\times10^{-4}$
A_2			$-9.7(5)\times10^{-9}$			$3.54(20)\times10^{-7}$	$-4.49(10)\times10^{-7}$	$-8.0(3)\times10^{-7}$	$5.8(5)\times10^{-6}$
A_3			$1.31(9)\times10^{-11}$						

https://doi.org/10.1154/1.1566957

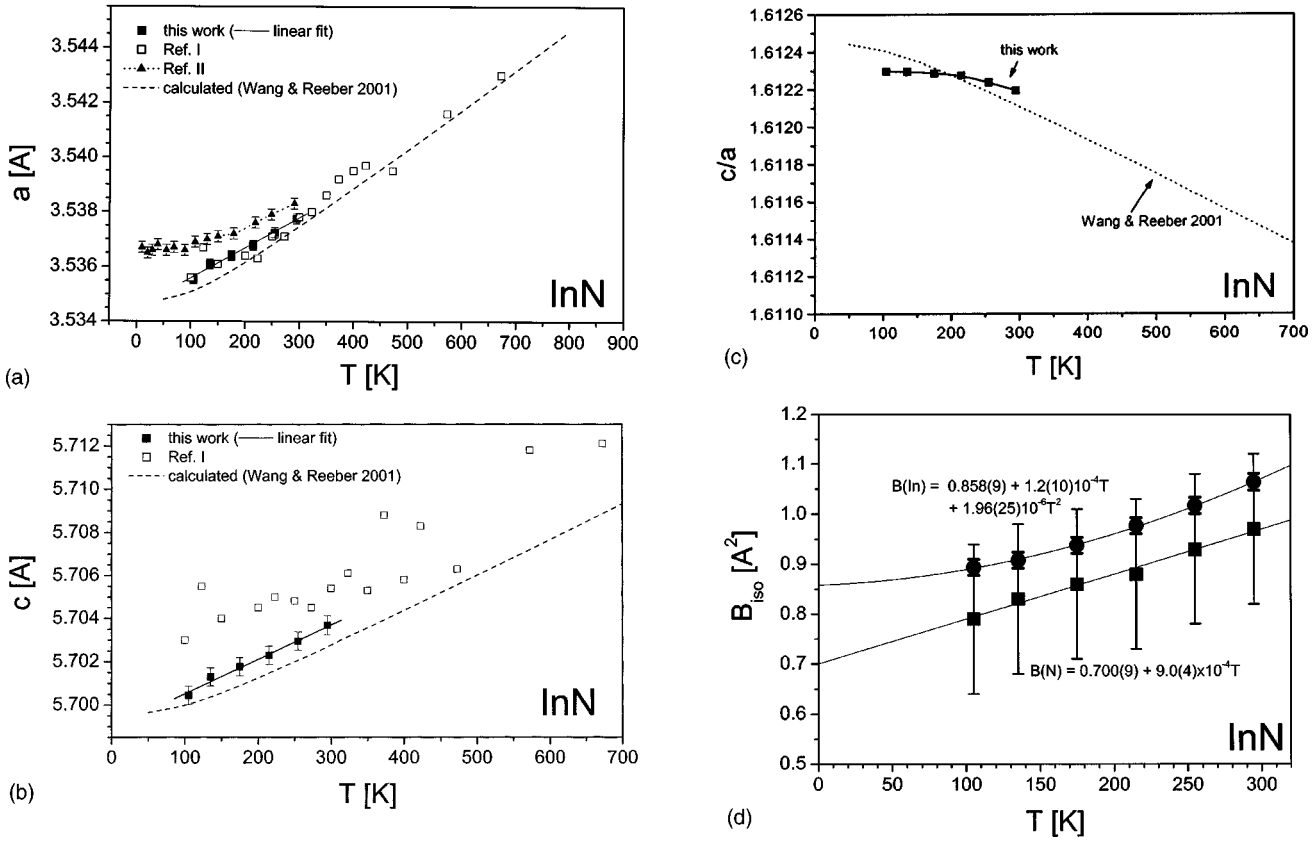

Figure 4. (a) and (b) Dependence of lattice-parameters, *a* and *c*, on temperature for indium nitride (squares). The solid lines represent polynomial fits of the experimental data. Earlier experimental (Ref. I, Ref. II) and calculated (Wang and Reeber, 2001) data are included. (c) Dependence of the axial ratio on temperature. Calculated data of Wang and Reeber (2001) are included for comparison. (d) Variation of the refined atomic displacement factors with temperature.

with increasing pressure. A similar behavior has been calculated for AlN (Christensen and Gorczyca, 1993).

The data from Ref. II presented in Figure 4 were collected for several selected reflections, resulting in a rather smooth dependence for lattice parameter *a*, but highly scattered points for lattice parameter *c* (not shown). (A high scatter of *c* values was also seen in Ref. I.) The $a(T)$ dependence is flattened at low temperatures, below about 100 K. The data of Ref. II are the first experimental indication that thermal expansion of InN tends to vanish at low temperatures. Further studies are needed to experimentally demonstrate such (expected) behavior for both *a* and *c* below ~100 K.

The TECs derived from the linear lattice parameters dependencies are $\alpha_a = 3.09(14) \times 10^{-6}$ K^{-1} and $\alpha_c = 2.79(16) \times 10^{-6}$ K^{-1}. A comparison with literature values is given in Table IV for a fixed temperature of 200 K. This temperature value was chosen because it constitutes the middle of the range studied in the present article. The results indicate that the thermal expansion in the basal plane is somewhat lower than that given in earlier papers, while that in the *c* direction is confirmed. Nevertheless, as the number of experimental points and the studied range were small, further studies (possibly employing synchrotron radiation) would yield more complete information on the thermal expansion of InN at low temperatures.

The lattice-parameter data (quoted in Table III) for the indium phase exhibit the known nonlinear behavior, as shown in Figure 5. However, some discrepancies with respect to the literature data were encountered. First, the lattice parameter *a* is larger while the lattice parameter *c* is smaller than those reported by Wolcyrz *et al.* (1981) and Flower and Saunders (1990). Second, the maximum at the temperature dependence of the lattice parameter *c* is shifted in relation to the literature data (Wołcyrz *et al.*, 1981; Flower and Saunders, 1990) by ΔT equal about 50 K towards lower temperatures. Also, the temperature variation of the parameter *a* is

TABLE IV. Comparison of experimental and calculated thermal-expansion coefficients at 200 K.

α_a (10^{-6} K^{-1})	α_c (10^{-6} K^{-1})	Remarks	Reference
3.45	2.72	experimental, nonlinear in the range 100–560 K	Sheleg and Savastenko (1976)
3.501	2.526	calculated, nonlinear in the range 50–800 K	Wang and Reeber (2001)
3.6(2)	2.6(3)	experimental, approximation by constants in the range 100–673 K	Paszkowicz *et al.* (1999)
3.09(14)	2.79(16)	experimental, approximation by constants in the range 105–295 K	this work

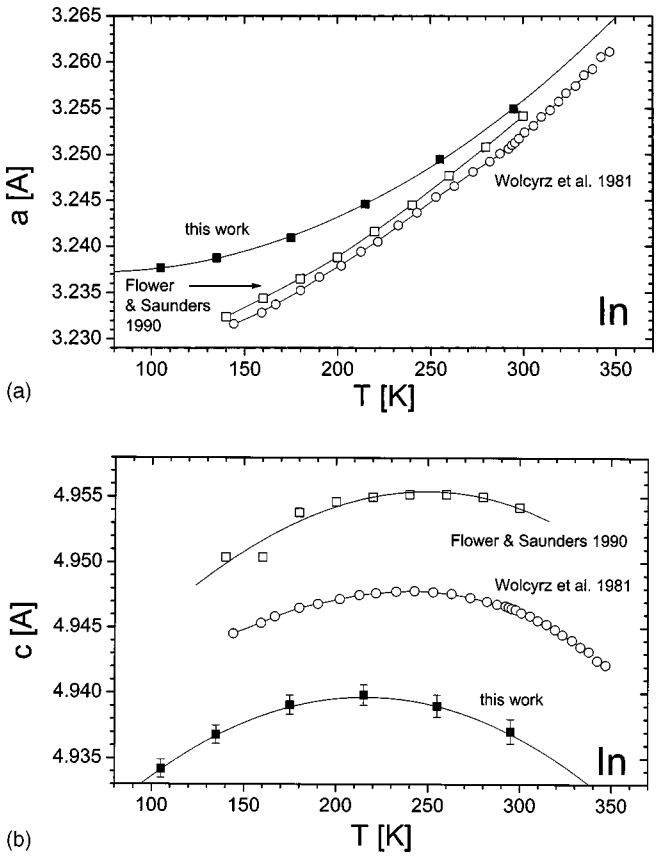

Figure 5. Dependence of lattice-parameters, *a* and *c*, on temperature for metallic indium (full squares). The line represents a polynomial fit. The errors for the *a* parameter are smaller than the symbol size. Literature data by Wołcyrz *et al.* (1981) and Flower and Saunders (1990) are shown for comparison (solid lines are a guide to the eye).

found to be somewhat different from the two literature datasets. Various factors may contribute to the above discrepancies in behavior, such as impurities in the indium phase (e.g., hypothetically dissolved nitrogen).

The present temperature dependencies are smooth for the main phase as well as for the secondary phase. This is in contrast to the results for InN obtained with the classical laboratory equipment (Ref. I), where insufficient counting statistics as well as possible sample displacement with temperature due to both, the sample holder construction and heating method, are thought to contribute to the observed scatter of experimental points.

IV. SUMMARY

Lattice parameters and TECs for InN microcrystals in the temperature range from 105 K up to 295 K were studied using X-ray powder diffraction at a synchrotron radiation source. The shape and face orientation of the elongated microcrystals were determined. It is shown that the dominant orientation of the long axis of the microcrystals is [001] while those for the side faces are (100) and (110). The lattice parameters of the studied sample at 295 K are $a=3.5377(2)$ Å, $c=5.7037(4)$ Å. In the studied temperature range, the TECs are $\alpha_a=3.09(14)\times10^{-6}$ K^{-1} and $\alpha_c=2.79(16)\times10^{-6}$ K^{-1}. The discussed dependencies of lattice parameters on temperature confirm the trends indicated earlier by data measured using conventional equipment and those obtained from calculations based on a semiempirical model. The free structural parameter, *u*, was experimentally determined. Its value at room temperature, 0.3769(13), agrees with earlier theoretical predictions; its variation with temperature is not conclusive because the changes are much smaller than the error margin. It may be concluded that application of a highly intense third-generation synchrotron source combined with a 2D position sensitive detector is advantageous for studies of thermal expansion.

ACKNOWLEDGMENTS

This work was supported in part within European Commission program ICA1-CT-2000-70018 (Center of Excellence CELDIS) and by Grant No. 7 T08A 053 19 from the State Committee for Scientific Research (Poland). Experimental assistance from the staff of the Swiss-Norwegian Beam Lines at ESRF is gratefully acknowledged.

Angus, J. C., Argoitia, A., Hayman, C. C., Wang, L., Dyck, J. S., and Kash, K. (**1997**). ''Growth of bulk polycrystalline gallium and indium nitride at subatmospheric pressures,'' Mater. Res. Soc. Symp. Proc., Vol. 468 (Materials Research Society, Pittsburgh) pp. 149–154.

Bechstedt, F., and Füller, J. (**2002**). ''Do we know the fundamental energy gap of InN?,'' J. Cryst. Growth **246**, 315–319.

Besson, J. M., Bellaiche, L., and Kunc, K. (**1996**). ''Second-order pretransitional effects in the high pressure phase transition of indium nitride,'' Phys. Status Solidi B **198**, 469–474.

Bhattacharya, P., Sharma, T. K., Singh, S., Ingale, A., and Kukreja, L. M. (**2002**). ''Observation of zincblend phase in InN thin films grown on sapphire by nitrogen plasma-assisted pulsed layer deposition,'' J. Cryst. Growth **236**, 5–9.

Bockowski, M. (**2001**). ''Growth and doping of GaN and AlN single crystals under high nitrogen pressure,'' Cryst. Res. Technol. **36**, 771–787.

Chichibu, S. F., Wada, K., Mullhauser, J., Brandt, O., Ploog, K. H., Mizutani, T., Setoguchi, A., Nakai, R., Sugiyama, M., Nakanishi, H., Korii, K., Deguchi, T., Sota, T., and Nakamura, S. (**2000**). ''Evidence of localization effects in InGaN single-quantum-well ultraviolet light-emitting diodes,'' Appl. Phys. Lett. **76**, 1671–1673.

Chisholm, J. A., Lewis, D. W., and Bristowe, P. D. (**1999**). ''Classical simulations of the properties of group-III nitrides,'' J. Phys.: Condens. Matter **11**, L235–L239.

Christensen, N. E., and Gorczyca, I. (**1993**). ''Calculated structural phase transitions of aluminum nitride under pressure,'' Phys. Rev. B **47**, 4307–4314.

Dyck, J. S., Kash, K., Hayman, C. C., Argoitia, A., Grossner, M. T., Angus, J. C., and Zhou, W. L. (**1999**). ''Synthesis of bulk polycrystalline indium nitride at subatmospheric pressures,'' J. Mater. Res. **14**, 2411–2417.

Elwell, D., Feigelson, R. S., Simkins, M. M., and Tiller, W. A. (**1984**). ''Crystal growth of GaN by the reaction between gallium and ammonia,'' J. Crypt. Growth **66**, 45–54.

Flower, S. C. and Saunders, G. A. (**1990**). ''The elastic behaviour of indium under pressure and with temperature up to the melting point,'' Philos. Mag. B **62**, 311–328.

Godlewski, M., and Goldys, E. M. (**2001**). ''Role of localisation effects in GaN and InGaN,'' in *Smart Optical Structures and Devices*, Proc. SPIE **4318**, 99–108.

Goryunova N. A. (**1965**). ''Chemistry of Diamond-type Semiconductors'' (WNT, Warsaw) (in Polish, translation from Russian edition).

Grzegory, I., Jun, J., Krukowski, S., Perlin, P., and Porowski, S. (**1993a**). ''InN thermodynamics and crystal growth at high pressure of N_2,'' Jpn. J. Appl. Phys., Suppl. **32-1**, 343–345.

Grzegory, I., Jun, J., Krukowski, S., Bockowski, M., and Porowski, S. (**1993b**). ''Crystal growth of III-N compounds under high nitrogen pressure,'' Physica B **185**, 99–102.

Grzegory, I., Krukowski, S., Jun, J., Bockowski, M., Wróblewski, M., and Porowski, S. (**1994**). ''Stability of indium nitride at N_2 pressure up to 20 kbar.'' AIP Conf. Proc. **309**, 565–568.
Hammersley, A. P. (**1995**). ''FIT2D V5.18 Reference Manual V1.6,'' ESRF Internal Report, EXP/AH/95-01.
Inushima, T., Mamutin, V. V., Vekshin, V. A., Ivanov, S. V., Motokawa, M., and Ohoya, S. (**2001**). ''Physical properties of InN with the band gap energy of 1.1 eV,'' J. Cryst. Growth **227–228**, 481–485.
Juza, R., and Hahn, H. (**1938**). ''On the crystal structure of Cu_3N, GaN and InN,'' Z. Anorg. Allg. Chem. **239**, 282 (in German).
Kim, C. C., Je, J. H., Ruterana, P., Degave, F., Nouet, G., Yi, M. S., Noh, D. Y., and Hwu, Y. (**2002**). ''Microstructures of GaN islands on a stepped sapphire surface,'' J. Appl. Phys. **91**, 4233–4237.
Kim, K., Lambrecht, W. R. L., and Segall, B. (**1996**). ''Elastic constants and related properties of tetrahedrally bonded BN, AlN, GaN, and InN,'' Phys. Rev. B **53**, 16310–16326.
Krukowski, S., Romanowski, Z., Grzegory, I., and Porowski, S. (**1998a**). ''Interaction of N_2 molecule with liquid Ga surface-quantum mechanical calculations (DFT),'' J. Cryst. Growth **189–190**, 159–156.
Krukowski, S., Witek, A., Adamczyk, J., Jun, J., Bockowski, M., Grzegory, I., Łucznik, B., Nowak, G., Wróblewski, M., Presz, A., Gierlotka, S., Stelmach, S., Pałosz, B., Porowski, S., and Zinn, P. (**1998b**). ''Thermal properties of indium nitride,'' J. Phys. Chem. Solids **59**, 289–295.
Kubota, K., Kobayashi, Y., and Fujimoto, K. (**1989**). ''Preparation and properties of III-V nitride thin films,'' J. Appl. Phys. **66**, 2984–2298.
Lee, H. C., Lee, K. Y., Yong, Y. J., Lee, J. Y., and Kim, G. H. (**1995**). ''Effect of hydrogen addition on the preferred orientation of AlN films prepared by reactive sputtering,'' Thin Solid Films **271**, 50–55.
Li, X. B., Sun, D. Z., Kong, M. Y., and Yoon, S. F. (**1998**). ''Structural identification of a cubic phase in hexagonal GaN films grown on sapphire by gas-source molecular beam epitaxy,'' J. Cryst. Growth **183**, 31–37.
Lima, A. P., Tabata, A., Leite, J. R., Kaiser, S., Schikora, D., Schöttker, B., Frey, T., As, D. J., and Lischka, K. (**1999**). ''Growth of cubic InN on InAs(001) by plasma-assisted molecular beam epitaxy,'' J. Cryst. Growth **201–202**, 396–398.
MacChesney, J. B., Bridenbaugh, P. M., and O'Connor, P. B. (**1970**). ''Thermal stability of indium nitride at elevated temperatures and nitrogen pressures,'' Mater. Res. Bull. **5**, 783–791.
Mamutin, V. V. (**1999**). ''Growth of $A^{III}N$ whiskers and plate-shaped crystals by molecular-beam epitaxy with the participation of the liquid phase,'' Tech. Phys. Lett. **25**, 741–744. (transl. from: Pisma Zhurn. Tekh. Fiz. 25, 55-63).
Miao, W. G., Wu, Y., and Zhou, H. P. (**1997**). ''Morphologies and growth mechanisms of aluminium nitride whiskers,'' J. Mater. Sci. **32**, 1969–1975.
Monemar, B. (**1999**). ''III-V nitrides—important future electronic materials,'' J. Mater. Sci.: Mater. Electron. **10**, 227–254.
Muñoz, A., and Kunc, K. (**1993**). ''Structure and static properties of indium nitride at low and moderate pressures,'' J. Phys.: Condens. Matter **5**, 6015–6022.
Nakamura, S. (**1999**). ''InGaN-based blue light-emitting diodes and laser diodes,'' J. Cryst. Growth **201–202**, 290–295.
Nakamura, S. (**2000a**). ''Role of alloy fluctuations in InGaN-based LEDs and laser diodes,'' Mater. Sci. Forum **338–342**, 1609–1614.
Nakamura, S. (**2000b**). ''Role of dislocations in InGaN-based LEDs and laser diodes,'' Int. J. High Speed Electron. **10**, 271–279.
Osamura, K., Naka, S., and Murakami, Y. (**1975**). ''Preparation and optical properties of $Ga_{1-x}In_xN$ thin films,'' J. Appl. Phys. **46**, 3432–3437.
Parala, H., Devi, A., Hipler, F., Maile, E., Birkner, A., Becker, H. W., and Fischer, R. A. (**2001**). ''Investigations on InN whiskers grown by chemical vapour deposition,'' J. Cryst. Growth **231**, 68–74.
Paszkowicz, W. (**1999**). ''X-ray powder diffraction data for indium nitride,'' Powder Diffr. **14**, 258–260.
Paszkowicz, W., Adamczyk, J., Krukowski, S., Leszczynski, M., Porowski, S., Sokolowski, J. A., Michalec, M., and Lasocha, W. (**1999**). ''Lattice parameters, density and thermal expansion of InN microcrystals grown by the reaction of nitrogen plasma with liquid indium,'' Philos. Mag. A **79**, 1145–1154.
Paszkowicz, W., and Knapp, M. (**1999**). Unpublished.
Paulus, B., Shi, F.-J., and Stoll, H. (**1997**). ''A correlated ab initio treatment of the zinc-blende wurtzite polytypism of SiC and III-V nitrides,'' J. Phys.: Condens. Matter **9**, 2745–2758.
Pichugin, I. G., and Tlachala, M. (**1978**). ''X-ray analysis of indium nitride,'' Inorg. Mater. **14**, 135–136 (translation from Izv. AN SSSR, Neorg. Mater. **14**, 175-176).
Podsiadlo, S. (**1995**). ''Stages of the synthesis of indium nitride with the use of urea,'' Thermochim. Acta **256**, 375–380.
Prywer, J., and Krukowski, S. (**1998**). ''GaN single crystal habits and their relation to GaN growth under high pressure of nitrogen,'' MRS Internet J. Nitride Semicond. Res. **3** (47), 1–10.
Rodriguez-Carvajal, J. (**2001**). ''Recent developments of the program FULLPROF,'' Newslett. IUCr Commission Powder Diffr. **26**, 12–19.
Romanowski, Z., Krukowski, S., Grzegory, I., and Porowski, S. (**2001**). ''Surface reaction of nitrogen with liquid group III metals,'' J. Chem. Phys. **114**, 6353–6363.
Sheleg, A.U., and Sevastenko, V.A. (**1976**) ''Investigation of thermal expansion of indium and gallium nitrides,'' Vestsi Akad. Navuk BSSR, No. 3, 126-128.
Stampfl, C., and Van de Walle, C.G. (**1999**) ''Density-functional calculations for III-V nitrides using the local-density approximation and the generalized gradient approximation,'' Phys. Rev. B **59**, 5521–5535.
Strite, S., Chandrasekhar, D., Smith, D. J., Sariel, J., Chen, H., Teraguchi, N., and Morkoç, H. (**1993**). ''Structural properties of InN films grown on GaAs substrates: observation of the zincblende polytype,'' J. Cryst. Growth **127**, 204–208.
Tabata, A., Lima, A. P., Teles, L. K., Scolfaro, L. M. R., Leite, J. R., Lemos, V., Schöttker, B., Frey, T., Schikora, D., and Lischka, K. (**1999**). ''Structural properties and Raman modes of zinc blende InN epitaxial layers,'' Appl. Phys. Lett. **74**, 362–364.
Tanaka, M., Nakahata, S. Sogabe, K., Nakata, H., and Tobioka, M. (**1997**). ''Morphology and X-ray diffraction peak widths of aluminum nitride single crystals prepared by the sublimation method,'' Jpn. J. Appl. Phys., Part 2 **36**, L1062–L1064.
Tansley, T. L. (**1994**). ''Crystal structure, mechanical properties, thermal properties and refractive index of InN,'' in *Properties of Group III Nitrides*, EMIS Datareviews Series, edited by J. H. Edgar (British Institution of Electrical Engineers Publ., London), pp. 35–40.
Tansley, T. L., and Foley, C. P. (**1986**). ''Optical band gap of indium nitride,'' J. Appl. Phys. **59**, 3241–3244.
Ueno, M., Yoshida, M., Onodera, A., Shimomura, O., and Takemura, K. (**1994**). ''Stability of the wurtzite-type structure under high pressure: GaN and InN,'' Phys. Rev. B **49**, 14–21.
Vaidhyanathan, B., Agrawal, D. K., and Roy, R. (**2000**). ''Novel synthesis of nitride powders by microwave-assisted combustion,'' J. Mater. Res. **15**, 974–981.
Wang, H. B., Han, J. C., Li, Z. Q., and Du, S. Y. (**2001**). ''Effect of additives on self-propagating high-temperature synthesis of AlN,'' J. Eur. Ceram. Soc. **21**, 2193–2198.
Wang, K., and Reeber, R. R. (**2001**). ''Thermal expansion and elastic properties of InN,'' Appl. Phys. Lett. **79**, 1602–1604.
Wołcyrz, M., Kubiak, R., and Maciejewski, S. (**1981**). ''X-ray investigation of thermal expansion and atomic thermal vibrations of tin, indium, and their alloys,'' Phys. Status Solidi B **107**, 245–253.
Wright, A. F., and Nelson, J. S. (**1995**). ''Consistent structural properties for AlN, GaN, and InN,'' Phys. Rev. B **51**, 7866–7869.
Wu, X. H., Kapolnek, D., Tarsa, E. J., Heying, B., Keller, S., Keller, B. P., Mishra, U. K., DenBaars, S. P., and Speck, J. S. (**1996**). ''Nucleation layer evolution in metal-organic chemical vapor deposition grown GaN,'' Appl. Phys. Lett. **68**, 1371–1373.
Wu, J., Walukiewicz, W., Yu, K. M., Ager, J. W., Haller, E. E., Lu, H., Schaff, W. J., Saito, Y., and Nanishi, Y. (**2002**). ''Unusual properties of the fundamental band gap of InN,'' Appl. Phys. Lett. **80**, 3967–3969.
Yeh, C.-Y., Lu, Z. W., Froyen, S., and Zunger, A. (**1992**). ''Zinc-blende-wurtzite polytypism in semiconductors,'' Phys. Rev. B **46**, 10086–10097.
Zhou, H. P., Chen, H., Liu, Y. C., and Wu, Y. (**2000**). ''Growth of aluminium nitride whiskers by sublimation-recrystallization method,'' J. Mater. Sci. **35**, 471–475.
Zoroddu, A., Bernardini, F., Ruggerone, P., and Fiorentini, V. (**2001**). ''First-principles prediction of structure, energetics, formation enthalpy, elastic constants, polarization, and piezoelectric constants of AlN, GaN, and InN: comparison of local and gradient-corrected density-functional theory,'' Phys. Rev. B **6404**, 045208/1-6.